Martian outer atmosphere is too low to permit any significant thermal escape, the possibility remains that the solar wind might sweep away some of the atmospheric gases. The observational evidence seems to oppose this. The outermost portion of the atmosphere must be atomic oxygen, and it would be mainly atomic oxygen that would be swept away by contact with the solar wind, leaving corresponding quantities of carbon monoxide in the atmosphere.

The failure to find spectroscopic evidence of carbon monoxide therefore indicates that the solar wind has not swept away any significant portion of the outer atmosphere. It is difficult to imagine any mechanism other than magnetic field that could protect the atmosphere from being partially swept away; this suggests that Mars may have a weak magnetic field, sufficient to divert the solar wind at some altitude exceeding a few hundred kilometers but not strong enough for detection by the magnetometers in Mariner IV. Alternatively, the magnetic field within the solar wind may be diverted by the Martian ionosphere, and this diversion may divert the solar wind and prevent any sweeping away of the Martian atmosphere.

The arguments for my model rest heavily on the spectroscopic evidence that carbon monoxide is not a prominent constituent of the Martian atmosphere. This factor indicates that atomic oxygen, formed by photodissociation of carbon dioxide, is not continually being swept away by the solar wind, carbon monoxide thus being permitted to accumulate. If the atomic oxygen is not rapidly removed, it must be a principal constituent of the Martian upper atmosphere, and its ions almost certainly must produce the principal band of ionization that was observed by Mariner IV.

F. S. JOHNSON

Earth and Planetary Sciences Laboratory, Southwest Center for Advanced Studies, Dallas, Texas

References and Notes

1. A. Kliore, D. L. Cain, G. S. Levy, V. R. Eshleman, G. Fjeldbo, F. D. Drake, *Science* **149**, 1243 (1965).
2. L. D. Kaplan, G. Munch, H. Spinrad, *Astrophys. J.* **139**, 1 (1964).
3. W. Sinton, *J. Quant. Spectry. Radiative Transfer* **3**, 551 (1963).
4. J. W. Chamberlain and D. M. Hunten, *Rev. Geophys.* **3**, 299 (1965).
5. T. Yonezawa, *J. Radio Res. Lab.* **5**, 165 (1958).
6. H. Rishbeth and D. W. Barron, *J. Atmospheric Terrest. Phys.* **18**, 234 (1960).
7. K. Rankama and Th. G. Sahama, *Geochemistry* (Univ. of Chicago Press, Chicago, 1950).

8. Supported by NASA grant NsG-269-62.

8 November 1965

Electron Density and Electronic Properties in Noble-Metal Transition Elements

Abstract. *It is shown empirically that the superconducting transition temperature as well as the magnetic susceptibility and the electronic specific heat of noble-metal transition elements and alloys can be described reasonably well as universal functions of the valence electron density, that is, the number of valence electrons per cubic centimeter.*

We have found that one can describe the electronic and magnetic behavior of all the noble-metal transition elements surprisingly well in terms of a single parameter—the electron density, that is, the number of valence electrons per cubic centimeter. This is quite a different concept from that of using valence electrons per atom as has previously been done (*1, 2*). In both cases the valence electrons are considered to be all those electrons outside the last filled shell. By plotting the superconducting transition temperature, the magnetic susceptibility, and the electronic specific heat against the electron density, we find universal functions of these properties for alloys both among the 4*d* and 5*d* elements as well as between them. Thus the difference between 4*d* and 5*d* alloys that otherwise showed up in similar plots in the past when the number of valence electrons per atom were used as a parameter can be accounted for by the difference in atomic volume.

Desorbo (*3*) had proposed a modification of the valence-electrons-per-atom rules (*1*) which took into account the difference in atomic volume of alloys with the same number of valence electrons per atom. He introduced an effective electron-per-atom ratio ($N_{\text{eff.}}$), which depended on the ratio of the atomic volumes of solute and solvent atoms. For alloys with the same solvent atom, his $N_{\text{eff.}}$ is also proportional to the electron density; his concept is, however, different from ours in that the constant of proportionality still depends on the volume of the solvent atom.

We have made a rather detailed investigation on the occurrence of superconductivity in alloys of noble-metal transition elements [Ir-rich alloys of the face-centered-cubic (fcc) phase] from 1.0 to 0.012°K. Our data are summarized in Fig. 1, in which we represent binary and ternary alloys in a two-dimensional way. The dashed lines indicate the various alloy systems which we have studied, namely the systems Os-Ir, Ir-Pt, Ir-Rh, Ir-Pd, Ir-Ru, $Ir_{0.8}Re_{0.2}$-Rh, $Ir_{0.7}Os_{0.3}$-Rh, and $Ir_{0.5}Rh_{0.5}$-Os. The scale on the *x*-axis in Fig. 1 represents the number of valence electrons per atom, namely 8 for Os and Ru, 9 for Ir and Rh, and 10 for Pt and Pd. Alloys with roughly equal transition temperatures are shown by a given symbol. The labeled solid lines are the approximate lines of constant transition temperature. In Fig. 2 we indicate in a similar plot

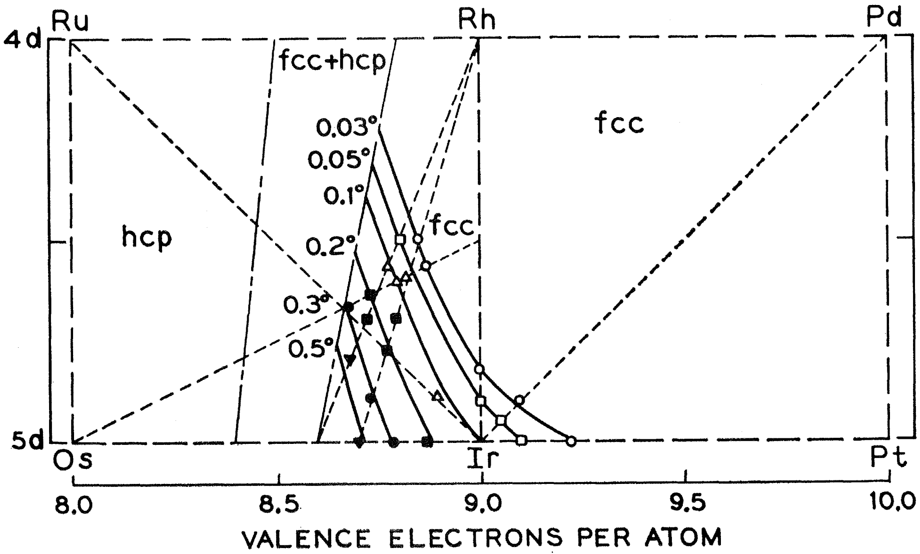

Fig. 1. Superconductivity in alloy systems of noble metals and transition elements. The dashed lines indicate the alloy systems investigated. The superconducting transition temperature of each alloy, represented by a point on a dashed line, is indicated roughly by the kind of symbol used for the point, namely 0.5° (▼), 0.3° (●), 0.2° (X), 0.1° (△), 0.05° (□), and 0.03° (○). The labeled solid lines are the approximate lines of constant transition temperature; *hcp*, hexagonal-close-packed; *fcc*, face-centered-cubic.

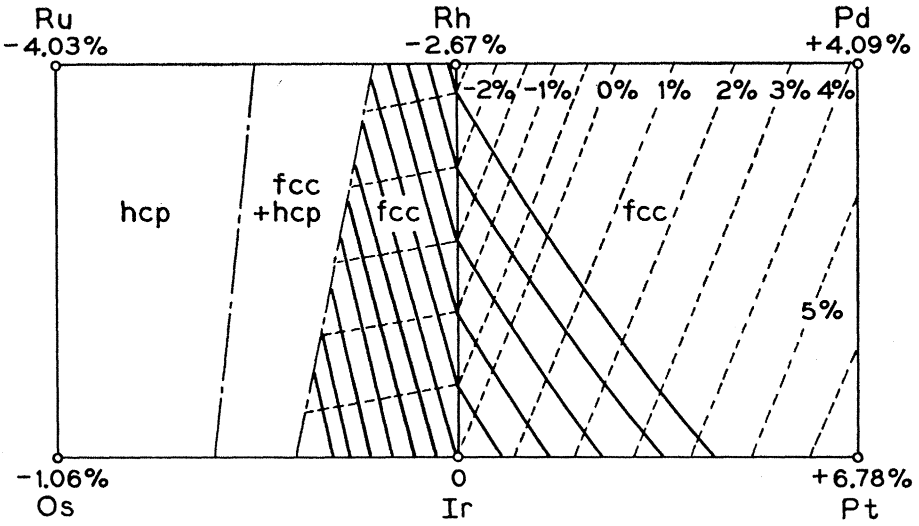

Fig. 2. Variation of atomic volume and electron density in face-centered-cubic (fcc) noble-metal transition elements and alloys. We have computed the data assuming the validity of Vegard's law and using room temperature values of lattice constants. The broken lines are lines of constant atomic volume, measured in the percentage deviation from the atomic volume of Ir (1.4143×10^{-23} cm^3). The solid lines are lines of constant electron density, plotted in steps of 0.5 percent deviation from the electron density of Ir ($6.363 \times 10^{+23}$ cm^3).

the variation of the mean atomic volume in the same alloy systems.

We have calculated the mean atomic volume on the basis of Vegard's law, according to which the lattice constant of an alloy varies linearly with the atomic ratio of the two (or more) elements in that alloy. Although this approximation is known to be very well obeyed in some of our alloy systems [Ir-Pd and Ir-Pt (*9*)] it is not always exact, and Fig. 2 may, therefore, contain systematic errors which, however, will not alter its general features. Generally, no deviation of Vegard's law will occur between elements of almost identical atomic volume.

We have normalized the atomic volume to the one of Ir (1.4143×10^{-23} cm^3), and we actually plot the percentage of deviation from it. The labeled dashed lines in Fig. 2 are lines of constant atomic volume. It should be noted that the successive increase in percentage in the atomic volume in the 4*d* metals Ru, Rh, and Pd is practically the same as the one in the 5*d* metals Os, Ir, and Pt. If Vegard's law is valid this then means that the atomic volume of each point in the fcc region in Fig. 2 is well defined, no matter in which particular alloy system of nearest-neighbor elements the point is considered.

By dividing the number of valence electrons of our alloys by their atomic volume we obtain the electron density; lines of constant electron density are shown by solid lines in Fig. 2. By comparison with Fig. 1, it can be seen that they follow quite well the lines of constant transition temperature. In Fig. 3, we have therefore plotted the logarithms of the superconducting transition temperatures against the electron density; within a certain scatter the points indeed follow a universal curve. In Fig. 3 we have also plotted all the known electronic specific heat and susceptibility data in units of density of states per electron volt and cubic centimeter (we plot

$$\chi/2\beta^2 \text{ and } \gamma/\frac{2\pi^2}{3}k_B{}^2,$$

β = Bohr magneton, χ = magnetic susceptibility, γ = electronic specific heat, and k_B = Boltzmann's constant, for the noble-metal transition elements and alloys in both the 4*d* and the 5*d* row.

Again it can be seen that the data can be described reasonably well by the electron density as a single parameter. Thus we see, for example, that the gigantic susceptibility of Pd as compared to that of Pt is a result consistent with this plot and seems to be only a consequence of Pd's larger electron density. It is interesting to note that the ferromagnetic elements Co and Ni, which are also fcc transition metals (3*d*), both have electron densities larger than that of Pd. If Au is added to Pt the susceptibility and the electronic specific heat drop rapidly. This might simply be due to the fact that adding Au to Pt decreases the electron density even if one assumes Au contributes 11 valence electrons per atom. If we had plotted the Pt-Au data on our graph (using 11 electrons per atom for Au) they would lie within 1 percent (in electron density) to the right of the present curves up to 20 percent (atoms) Au.

From our results (Fig. 3) we are led to conclude that superconductivity in Rh and Pt will occur below 0.001°K,

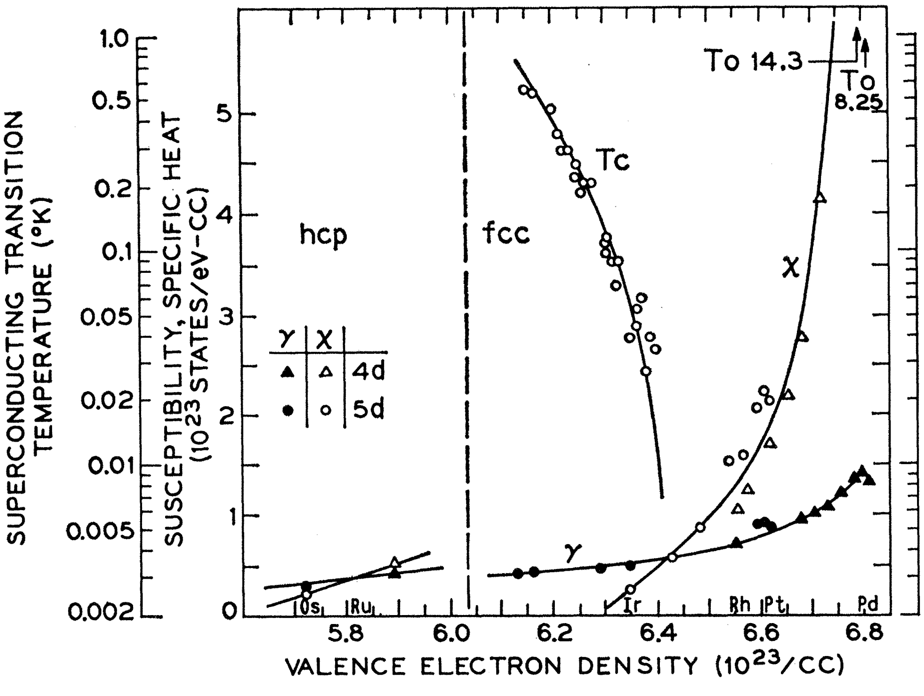

Fig. 3. Superconducting transition temperature, magnetic susceptibility, and electronic specific heat of noble-metal transition elements and alloys, plotted against electron density. The data on electronic specific heat and magnetic susceptibility, plotted in units of density of states per electron volt and cubic centimeter, are taken from Beck (*2*).

if at all; and that Pd will apparently not superconduct, as has been predicted theoretically by Doniach (*5*). Apparently the disappearance of the superconductivity is intimately connected with the appearance of the high susceptibility. That such a relationship should exist was first pointed out by Clogston (*6*), and later by Doniach (*5*), and is a consequence of the fact that the interactions which enhance the susceptibility also affect the superconductivity.

M. Anthony Jensen
University of California, La Jolla
B. T. Matthias
University of California, La Jolla,
and Bell Telephone Laboratories,
Murray Hill, New Jersey
K. Andres
Bell Telephone Laboratories,
Murray Hill

References and Notes

1. B. T. Matthias, *Progress in Low Temperature Physics*, C. J. Gorter, Ed. (North-Holland, Amsterdam, 1957), vol. 2, p. 138.
2. P. A. Beck, *The Electronic Structure and Alloy Chemistry of the Transition Elements* (Wiley, New York, 1963), p. 29.
3. W. Desorbo, *Phys. Rev.* **130**, 2177 (1963).
4. E. Raub and W. Plate, *Z. Metallk.* **47**, 688 (1956); ———, *ibid.* **48**, 444 (1957).
5. S. Doniach, Contribution to Manchester Many-Body Conference, Manchester, England, September 1964. We thank Dr. Doniach for sending us a copy of this paper.
6. A. M. Clogston, V. Jaccarino, Y. Yafet, *Phys. Rev.* **134**, A650 (1964).
7. We thank T. H. Geballe, L. J. Sham, and S. Gygax for discussions, Mrs. V. B. Compton for determining some of the lattice constants and for her help in obtaining the data used for Fig. 2, and H. L. Luo and E. Corenzwit for preparing some of the samples. One of us (M.A.J.) thanks J. M. Goodkind for technical advice on building a low-temperature apparatus and T. F. Smith, R. A. Simpkins, S. B. Sears, R. E. Siemon, and B. R. Maple for building the apparatus. Some of the work reported was taken from a theses (M.A.J.) presented to the University of California, La Jolla, in partial fulfillment of the Ph.D. requirement.

24 November 1965

■

Comparison of Messenger RNA in Photoperiodically Induced and Noninduced Xanthium Buds

Abstract. *In response to the floral stimulus,* Xanthium *buds synthesize relatively more messenger RNA than do vegetative buds. This is demonstrated by fractionation, on methylated albumin–kieselguhr columns, of a mixture of nucleic acids from vegetative and induced buds, one being labeled with uridine-*H^3 *and the other with uridine-2-*C^{14}*. While floral induction stimulates a small increase in messenger RNA synthesis as revealed by labeling intact plants, this difference can be magnified by labeling excised buds in solution. From experiments with excised buds from* Xanthium *plants, it is concluded that buds from photoperiodically induced plants contain more messenger RNA than buds from noninduced ones do.*

Messenger RNA (mRNA) serves as the intermediate in the translation of the informational strand of DNA into protein molecules (*1*). Thus, the biological activities of a cell are a reflection of its enzymes, and its enzymes in turn are reflected by various RNA messengers. Therefore, the regulation of biological activities by environmental influences might be expected to result in an altered frequency of enzymes produced as well as RNA messengers. Spiegleman and Hayashi (*1*), using both bacteria and bacterial virus, have demonstrated qualitative differences in the synthesis of RNA during different times of growth of bacteria or different stages of infection by virus. They demonstrated differences in the labeling of mRNA's from two populations of bacteria or virus by labeling the RNA with either uridine-H^3 or uridine-C^{14} at different times and then fractionating a mixture of both RNA's on a methylated albumin–kieselguhr (MAK) column. There is little or no other information on differences in the types of RNA messengers in biological tissue except for changes in mRNA during seed germination (*2*) and variation in chromosomally directed protein synthesis from different parts of the pea plant (*3*). For other higher plants, there is no information available on this subject even though there are many instances in which changes in the environment specifically lead to the induction of enzymes or changes in cellular differentiation. The photoperiodic induction of *Xanthium* plants, for development of floral primordia by a single long night (16 hours of darkness), is an example of such an environmental control. Exposure of a *Xanthium* plant to a 16-hour period of darkness initiates the production of the flowering hormone in the mature leaf, and when it has been transported to the apex it causes the vegetative bud to grow into a reproductive bud (*4*). These changes are probably hormonal controls acting as gene corepressors or coactivators. At the onset of floral induction there may be changes in the species of mRNA produced or perhaps an increase in the relative frequency of some new mRNA's over others.

Changes in RNA synthesis in the *Xanthium* plant were investigated with a specific aim of determining whether floral induction causes the synthesis of different amounts or types of mRNA's. By means of double-labeling technique and fractionation of the nucleic acids on MAK columns, it was found that buds of photoperiodically induced plants contain more mRNA.

Seeds of *Xanthium pensylvanicum* Wall. (cocklebur) were washed in running tap water for 3 days and then germinated in vermiculite. The seedlings were transplanted and grown in a controlled-environment greenhouse. The day length was maintained at 18 hours with supplementary light, and the temperature was maintained at approximately 23°C during the day and 17°C at night. The plants were grown in this environment for approximately 6 weeks. At the beginning of each experiment, the plants were defoliated except for a single leaf, which was usually the third leaf from the apex (approximately 7 cm long). The plants were randomly selected and placed in either of two growth chambers. One growth chamber was regulated for 8 hours of light and 16 hours of darkness (short day, SD) while the second was set for 16 hours of light and 8 hours of darkness (long day, LD). In both chambers, the temperature was kept at 27°C during the light period and at 18°C during the dark period. These conditions were satisfactory to control photoperiodic induction; a single inductive period (16 hours of darkness) would result in the development of floral primordia (*5*).

In order to compare the RNA synthesized in the apical buds of *Xanthium* plants, the apices of either intact or excised buds were labeled with uridine-H^3 or uridine-2-C^{14}. In experiments where the intact buds were labeled, a drop of either uridine-H^3 (20 μc) or uridine-2-C^{14} (1 μc) was applied to the apex of the plant 16 hours prior to harvesting. In other experiments, buds (2 to 3 mm in length)